

11-1-2005

Variation in the carotid bifurcation geometry of young versus older adults: Implications for geometric risk of atherosclerosis

Jonathan B. Thomas
Robarts Research Institute

Luca Antiga
Robarts Research Institute

Susan L. Che
Robarts Research Institute

Jaques S. Milner
Robarts Research Institute

Dolores A.Hangan Steinman
Robarts Research Institute

See next page for additional authors

Follow this and additional works at: <https://ir.lib.uwo.ca/medpub>

Citation of this paper:

Thomas, Jonathan B.; Antiga, Luca; Che, Susan L.; Milner, Jaques S.; Steinman, Dolores A.Hangan; Spence, J. David; Rutt, Brian K.; and Steinman, David A., "Variation in the carotid bifurcation geometry of young versus older adults: Implications for geometric risk of atherosclerosis" (2005). *Department of Medicine Publications*. 281.
<https://ir.lib.uwo.ca/medpub/281>

Authors

Jonathan B. Thomas, Luca Antiga, Susan L. Che, Jaques S. Milner, Dolores A. Hangan Steinman, J. David Spence, Brian K. Rutt, and David A. Steinman

Variation in the Carotid Bifurcation Geometry of Young Versus Older Adults

Implications for Geometric Risk of Atherosclerosis

Jonathan B. Thomas, MSc; Luca Antiga, PhD; Susan L. Che, BSc; Jaques S. Milner, BSc;
Dolores A. Hangan Steinman, MD, PhD; J. David Spence, MD;
Brian K. Rutt, PhD; David A. Steinman, PhD

Background and Purpose—Retrospective analysis of clinical data has demonstrated major variations in carotid bifurcation geometry, in support of the notion that an individual's vascular anatomy or local hemodynamics may influence the development of atherosclerosis. On the other hand, anecdotal evidence suggests that vessel geometry is more homogenous in youth, which would tend to undermine this geometric risk hypothesis. The purpose of our study was to test whether the latter is indeed the case.

Methods—Cross-sectional images of the carotid bifurcations of 25 young adults (24 ± 4 years) and a control group of 25 older subjects (63 ± 10 years) were acquired via MRI. Robust and objective techniques were developed to automatically characterize the 3D geometry of the bifurcation and the relative dimensions of the internal, external, and common carotid arteries (ICA, ECA, and CCA, respectively).

Results—Young vessels exhibited significantly less interindividual variation in the following geometric parameters: bifurcation angle ($48.5 \pm 6.3^\circ$ versus $63.6 \pm 15.4^\circ$); ICA angle ($21.6 \pm 6.7^\circ$ versus $29.2 \pm 11.3^\circ$); CCA tortuosity (0.010 ± 0.003 versus 0.014 ± 0.011); ICA tortuosity (0.025 ± 0.013 versus 0.086 ± 0.105); ECA/CCA diameter ratio (0.81 ± 0.06 versus 0.75 ± 0.13), ICA/CCA (0.81 ± 0.06 versus 0.77 ± 0.12) diameter ratio, and bifurcation area ratio (1.32 ± 0.15 versus 1.19 ± 0.35).

Conclusions—The finding of more modest interindividual variations in young adults suggests that, if there is a geometric risk for atherosclerosis, its early detection may prove challenging. Taken together with the major interindividual variations seen in older vessels, it suggests a more complex interrelationship between vascular geometry, local hemodynamics, vascular aging, and atherosclerosis, the elucidation of which now calls for prospective studies. (*Stroke*. 2005;36:2450-2456.)

Key Words: atherosclerosis ■ carotid artery ■ hemodynamics ■ MRI ■ aging

The observation that atherosclerotic plaques tend to occur near arterial bifurcations and bends has led to the widely accepted notion that hemodynamic forces play an important role in the development and progression of atherosclerosis.¹ Because these forces are determined primarily by vessel geometry, it has been suggested that certain individuals might be at higher risk of developing atherosclerosis by virtue of their particular vascular geometry.² An early study showed little difference between branch diameters and angles measured from planar angiograms of normal and diseased carotid arteries;³ however, subsequent studies of a variety of branching vessels, including the carotid bifurcation, have lent qualified support to this geometric risk hypothesis.⁴⁻⁹

Central to the notion of geometric risk for atherosclerosis is the assumption that vessel geometry varies sufficiently widely across the population. A recent analysis of angiograms from nearly 3000 patients in the European Carotid Surgical Trial (ECST) showed convincingly that there were major interindividual variations in the diameter and area ratios of the carotid bifurcation.¹⁰ However, despite attempting to minimize the secondary effects of disease on geometry by excluding vessels with $\geq 30\%$ stenosis, the authors conceded that early atheromatous changes not detectable in conventional angiograms might have led to an overestimation of the anatomic variation. That this may have been the case is suggested by routine clinical experience that dilated and

Received June 29, 2005; accepted August 4, 2005.

From the Imaging Research Laboratories (J.B.T., L.A., S.L.C., J.S.M., D.A.H.S., B.K.R., D.A.S.) and the Stroke Prevention and Atherosclerosis Research Center (J.D.S.), Robarts Research Institute, London, Ontario, Canada; the Department of Medical Biophysics (J.B.T., S.L.C., B.K.R., D.A.S.), University of Western Ontario, London, Ontario, Canada; and the Bioengineering Department (L.A.), Mario Negri Institute for Pharmacological Research, Bergamo, Italy.

J.B.T. and L.A. contributed equally to this work.

Correspondence to David A. Steinman, PhD, Imaging Research Laboratories, Robarts Research Institute, 100 Perth Dr, P.O. Box 5015, London, Ontario, Canada N6A 5K8. E-mail steinman@imaging.robarts.ca

© 2005 American Heart Association, Inc.

Stroke is available at <http://www.strokeaha.org>

DOI: 10.1161/01.STR.0000185679.62634.0a

tortuous carotid arteries are more frequent in older versus young subjects. Hence, toward our goal of elucidating the relationship between vascular hemodynamics and atherosclerosis, we set out to test, quantitatively, the hypothesis that the carotid bifurcations of young adults, indeed, exhibit less interindividual variability than those of older subjects.

Methods

The young group consisted of 25 ostensibly healthy volunteers (24 ± 4 years; range, 19 to 38 years; 14 M:11 F). A control group of 25 older subjects (63 ± 10 years; range, 42 to 75 years; 12 M:13 F) was recruited from among asymptomatic patients being followed at the Stroke Prevention and Atherosclerosis Research Centre (London). The inclusion criteria were $\leq 30\%$ stenosis bilaterally based on prior duplex ultrasound examination and no contraindications for MRI. The ethics review board of our university approved the experimental protocol, and all of the subjects gave informed consent.

Baseline demographic characteristics of the older group were as follows: 14 (56%) were hypertensive, 4 (16%) had diabetes mellitus, 1 (4%) was a current smoker, 5 (20%) were exsmokers, BMI was 27.6 ± 2.8 kg/m², total cholesterol was 5.44 ± 1.17 mmol/L, triglycerides were 1.97 ± 1.81 mmol/L, and total plaque area¹¹ was 0.881 ± 0.611 cm². Demographic data were not collected for the young group.

Imaging and Lumen Reconstruction

MRI was performed on a 1.5-T Signa scanner (GE Medical Systems) using bilateral phased array coils. After localization, both carotid bifurcations were imaged simultaneously with a peripherally gated black blood MRI protocol, which acquired, on average, 28×2 -mm-thick, transverse, contiguous slices with 0.313-mm nominal in-plane resolution. Scan parameters included 2D fast-spin echo, 8-cm-thick superior and inferior saturation bands, 160×160 mm² field-of-view, 512×384 acquisition matrix, 2R-R repetition time, 15 ms echo time, and 4 echo train length. Total acquisition time, including the initial localizing scan, was typically 15 minutes per subject.

Lumen boundaries for the left and right common, internal, and external carotid arteries (CCA, ICA, and ECA, respectively) were extracted from each of the black blood images using a semiautomated technique.¹² Distal branches of the ECA were excluded because of their small size. The resulting stack of contours was automatically converted into a binary image volume, within which a 3D discrete dynamic contour¹³ was inflated to define the 3D lumen geometry. Additional details of the imaging and digital reconstruction of the carotid bifurcation are provided elsewhere.¹⁴

Geometric Characterization

Once digitally reconstructed, each 3D lumen geometry was subjected to a novel, fully automated geometric characterization. In past studies, vessel dimensions and ratios have been measured at a variety of locations, typically defined in terms of some nominal distance from a user-identified landmark like the bifurcation apex and often varying in definition from study to study. In the present study, we sought to make measurements based on more rigorous and objective criteria, both to minimize operator bias and to encourage standardization of geometric definitions for future studies.

As illustrated in Figure 1A, centerlines were first generated from the CCA to each of the ICA and ECA branches. According to their definition, each centerline hosts the centers of spheres of maximal radius inscribed in the vessel. (In practice, the diameter of a maximally inscribed sphere approximates the minimum diameter of the vessel.) These centerline tracts and their associated sphere radii were then used to identify the origin and nominal plane of the bifurcation and to split the vessel into its 3 constituent branches.¹⁵ Geometric characterization then proceeded with respect to this vessel-specific coordinate system.

To define objective geometric parameters for bifurcations having different shapes and sizes, we first defined a distance metric along the centerlines based on the maximally inscribed spheres. As

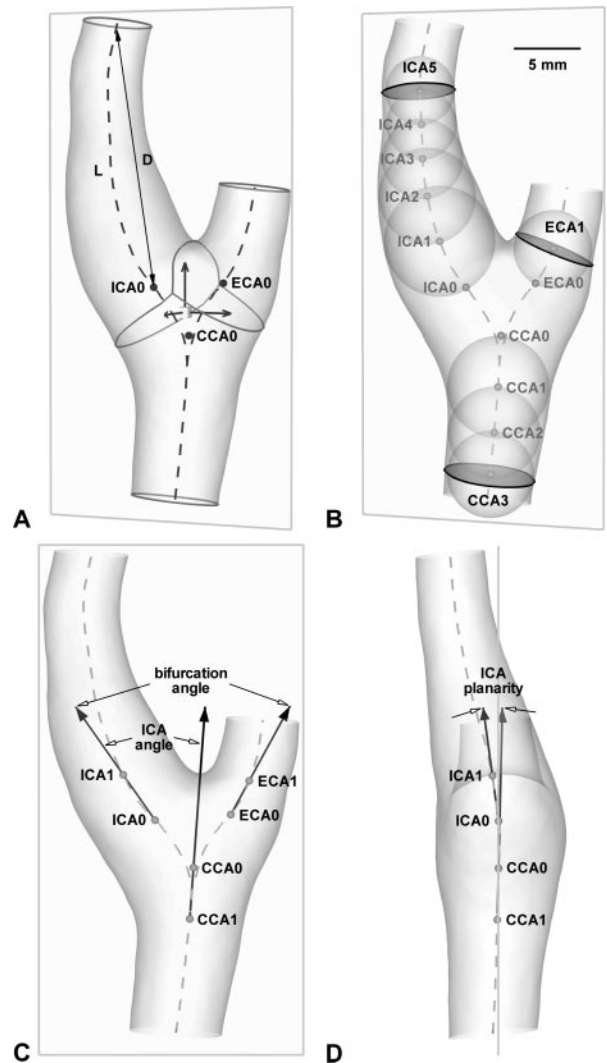


Figure 1. Definition of geometric parameters. (A) digitally reconstructed carotid bifurcation with branch divisions (solid lines) and centerlines (dashed lines); bifurcation origin (cube), coordinate axes (arrows), and plane (surrounding rectangle); and origins of the common, internal, and external carotid artery branches (CCA0, ICA0, and ECA0, respectively). Shown also are the ICA centerline length (L) and linear distance (D), used to calculate branch tortuosity. (B) maximally inscribed spheres used to define distances along vessel centerlines and planes from which branch areas and diameters were computed. (C and D) Vectors used to calculate various angles in views normal and tangent to the bifurcation plane respectively.

illustrated in Figure 1B, starting from each centerline origin (ie, CCA0, ICA0, and ECA0) and moving away from the bifurcation, the center of the maximally inscribed sphere tangent to the respective point was identified (ie, CCA1, ICA1, and ECA1). Repeating this process produced a series of points spaced 1 sphere radius apart, thus providing a robust and objective analog to the common practice of identifying vessel locations based on an integral number of nominal vessel diameters or radii.

To compute the mutual angles of the branches coming off the bifurcation, branch orientations were first defined as the vectors extending from the branch origins (CCA0, ICA0, and ECA0) to a point 1 sphere radius distal (CCA1, ICA1, and ECA1, respectively). As illustrated in Figure 1C, the bifurcation angle was then defined simply as the angle between the projections of the ICA and ECA vectors onto the bifurcation plane. Similarly, the ICA angle was defined as the angle between the projections of CCA and ICA

vectors onto the bifurcation plane, whereas ICA planarity was defined as the angle between the out-of-plane components of the CCA and ICA vectors (Figure 1D).

Vessel tortuosity was calculated as $L/D-1$, where, as illustrated for the ICA in Figure 1A, L is the length of the centerline from the origin to the end of the branch, and D is the Euclidean distance between these 2 points. Tortuosity may, therefore, be thought of as the fractional increase in length of the tortuous vessel relative to a perfectly straight path. Thus, a tortuosity of 0.0 corresponds to a perfectly straight vessel, whereas a tortuosity of, say, 0.2 identifies a vessel 20% longer than the shortest distance between 2 points.

To facilitate comparison with the diameter and area data of Schulz and Rothwell,¹⁰ cross-sectional areas and diameter were identified as far as possible away from the bifurcation. Because of the reduced axial coverage available from our particular MRI protocol, it was not always possible to measure these at locations consistent with that study, namely, where the vessel walls are parallel. Instead, we simply defined consistent distances, in terms of our sphere-radius-based distance metric, where the cross-sectional areas were computed. As illustrated in Figure 1B, these were placed at points CCA3, ICA5, and ECA1. (These locations were chosen to be consistent with those used by Goubergrits et al.^{16,17} in their studies of carotid bifurcation.) Cross-sectional areas were defined by the intersection of each branch surface with planes normal to centerlines at these respective points. The bifurcation area ratio was calculated as the sum of the ICA and ECA areas, divided by the CCA area. ICA/CCA, ECA/CCA, and ECA/ICA diameter ratios were calculated as the square root of the respective area ratios, equivalent to assuming that the (typically noncircular) vessel cross-sections were circles of equivalent area.

The combined effect of scan-to-scan and operator variability on the precision of the digital lumen reconstructions has been assessed previously via repeated imaging and analysis of 3 elderly subjects each imaged 3 times each at weekly intervals.¹⁸ Reproducibility of

the geometric parameters was similarly assessed here using the digital reconstructions from that study.

Statistical Analysis

For each geometric parameter, groups were compared by 2-way nested ANOVA. Two factors were identified as potential sources of interindividual variation in the data, namely age group (young versus older) and gender, and so the interaction between these was included. Nesting was introduced to account for the fact that each subject contributed 2 vessels to the data. Because some of the dependent geometric variables (bifurcation angle, CCA tortuosity, and ICA tortuosity) presented different SDs between age groups (ratio >4), an inverse transformation was applied to correct for their unequal variances before the analysis. A systematic comparison of the variances of the 2 age groups was performed by means of F tests, for which vessels were pooled into the same age group irrespective of gender. Within the older group, the effect of baseline demographic data on each geometric parameter was similarly tested using nested ANOVA. All of the statistical analyses were performed using the open-source R language and environment for statistical computing (version 1.9). Significance was assumed at a level of $P=0.05/9=0.0056$, reflecting the usual value corrected, according to the Bonferroni procedure, by the number of geometric parameters tested.

Results

The complete set of reconstructed carotid bifurcation lumen geometries for the young and older groups is presented in Figures 2 and 3, respectively. The young carotid bifurcation is clearly seen to exhibit much less geometric variation compared with the older subjects, and this is corroborated by the descriptive statistics for the geometric parameters summarized in Table 1. In particular, F-tests revealed that

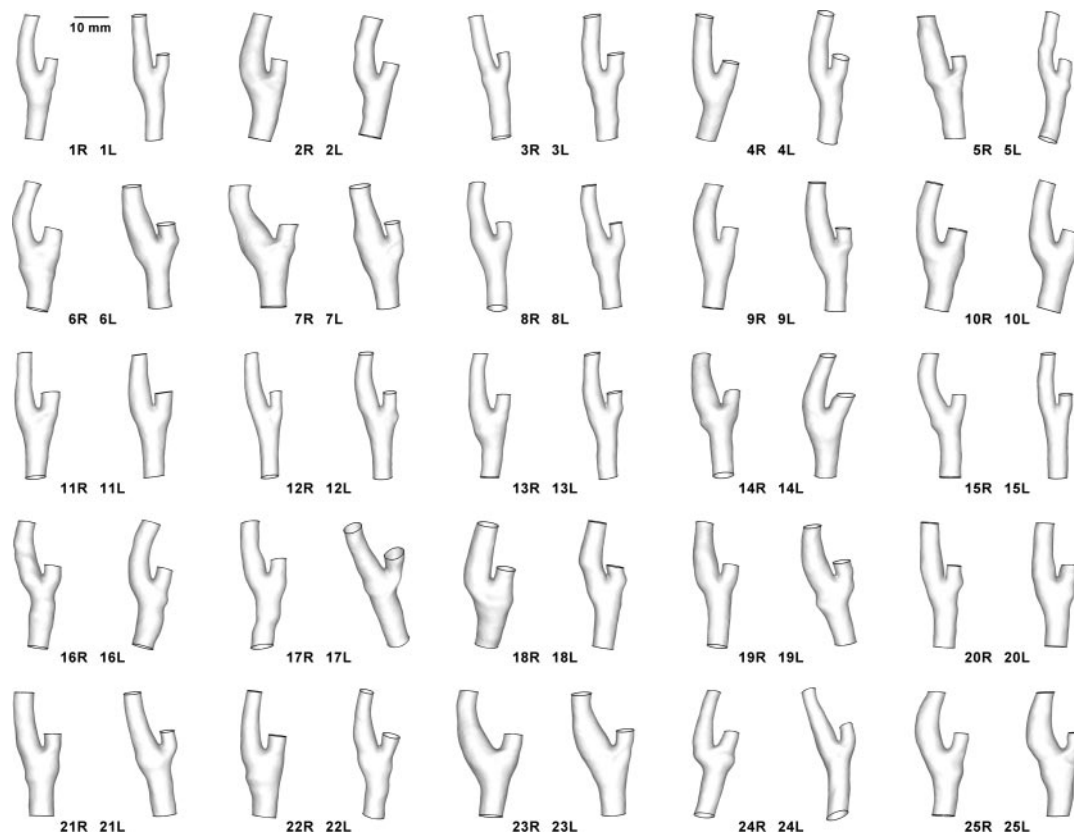


Figure 2. Carotid bifurcations digitally reconstructed from black blood MRI of young adults. Right and left vessels are presented together for each subject, numbered 1 to 25. All of the vessels are shown to the same scale, and rotated to their respective bifurcation planes. Orientation of each vessel relative to the body axis may be inferred from the angulation of vessel ends.

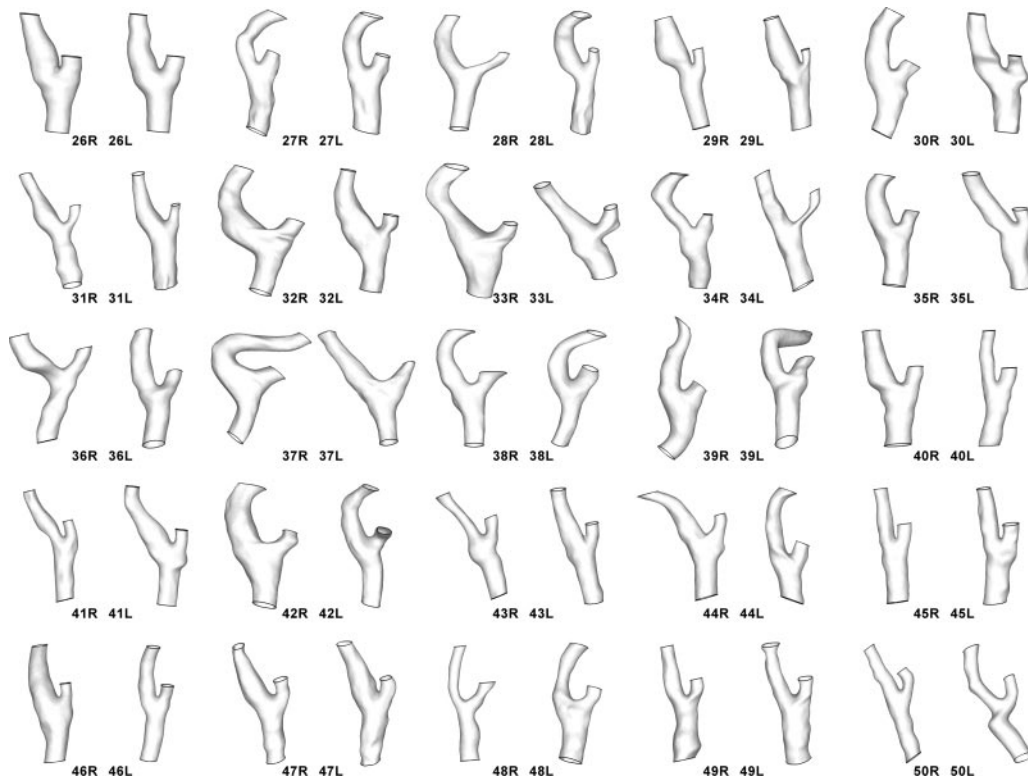


Figure 3. Carotid bifurcations digitally reconstructed from black blood MRI of older subjects, numbered 26 to 50. Refer to caption of Figure 2 for additional details.

interindividual variations in the young carotid bifurcation geometries were significantly lower than those for the older group. ANOVA revealed that age grouping (ie, young versus older) had a significant effect on the bifurcation angle, ICA angle, and CCA tortuosity. Within the older group, there were no significant effects of baseline demographics on the geometric parameters using the conservative Bonferroni-corrected P value of 0.0056; however, there was a near-significant effect of total plaque area on the ICA:CCA diameter ratio ($P=0.0095$) and the related bifurcation area ratio ($P=0.0058$).

Finally, as summarized in Table 2, geometric parameters were highly reproducible, with SDs well below the respective interindividual variations observed for the older group and near or below those of the young group.

Discussion

Our study confirms that there are, indeed, major geometric variations in the carotid bifurcation geometries of older subjects with little or no carotid artery disease; however, younger vessels exhibit significantly less geometric variability. This quantitatively supports anecdotal evidence indicating the relative homogeneity of vessel geometry in young versus older subjects. It also suggests that data from the ECST study may, indeed, have been confounded by the secondary effects of atherosclerosis. The recent finding of an association between intimal thickening and ICA angle of origin⁹ may also have been confounded by the effects of atherosclerosis, because our companion study of carotid bifurcation anthropometrics showed that orientation of the

carotid bifurcation relative to the sagittal plane of the body (a quantity related to ICA angle of origin) was significantly less variable within the young versus older group.¹⁹

Potential Shortcomings

Despite that fact that strong significant differences were seen between the 2 groups, it remains that our sample size was nearly 2 orders of magnitude smaller than that used to characterize geometric variability in the ECST study. Nevertheless, F-tests revealed no significant difference between our SDs and those derived from the ECST study, except for the case of area ratio ($P<0.0001$). Unpaired t tests did reveal that our mean diameter and area ratios were significantly higher ($P<0.0001$); however, this may be attributed to the relatively limited axial coverage of our black blood MRI protocol. To demonstrate this, we computed diameter and area ratios from a detailed survey of carotid bifurcation diameters²⁰ and found that ratios derived from proximal sites roughly corresponding to ours were similarly higher than those derived from distal sites more closely matching those defined for the ECST study: 0.78 versus 0.71 (ICA/CCA); 0.75 versus 0.53 (ECA/CCA); 0.97 versus 0.75 (ECA/ICA); and 1.17 versus 0.77 (area ratio).

This effect of the choice of measurement site may also be seen in the broader comparison of our data with those of the ECST study and postmortem measurements of Goubergrits et al.^{16,17} presented in Figure 4: our measurements were deliberately made at locations comparable to those used in the latter studies, and it can be seen that their diameter and area ratios are comparable to those of our older group. F tests

TABLE 1. Descriptive Statistics for Geometric Parameters

Geometric Parameter	Group	n	Mean	SD	Minimum*	Maximum*
Bifurcation angle	Young	50	48.5°	6.3°	39.7° (8L)	65.8° (25L)
	Older	50	63.6°	15.4°	31.2° (26R)	97.6° (37R)
	Young vs older		$P<0.0001$	$P<0.0001$		
ICA angle	Young	50	21.6°	6.7°	10.8° (13R)	39.1° (23R)
	Older	50	29.2°	11.3°	1.8° (43R)	62.7° (32R)
	Young vs older		$P=0.0002$	$P=0.0004$		
ICA planarity	Young	50	7.0°	4.8°	0.1° (1R)	21.6° (18R)
	Older	50	8.5°	8.1°	0.2° (42R)	42.8° (36R)
	Young vs older		$P=0.22$	$P=0.0003$		
CCA tortuosity	Young	50	0.010	0.003	0.004 (15L)	0.021 (16R)
	Older	50	0.014	0.011	0.005 (26L)	0.063 (50L)
	Young vs older		$P=0.0022$	$P<0.0001$		
ICA tortuosity	Young	50	0.025	0.013	0.006 (3R)	0.055 (25R)
	Older	50	0.086	0.105	0.007 (29L)	0.521 (37R)
	Young vs older		$P=0.049$	$P<0.0001$		
ICA:CCA	Young	50	0.81	0.06	0.69 (24L)	0.94 (5R)
	Older	45	0.77	0.12	0.52 (48R)	1.04 (35R)
	Young vs older		$P=0.077$	$P<0.0001$		
ECA:CCA	Young	50	0.81	0.06	0.70 (8L)	0.95 (4R)
	Older	46	0.75	0.13	0.50 (31R)	1.10 (37L)
	Young vs older		$P=0.040$	$P<0.0001$		
ECA:ICA	Young	50	1.00	0.11	0.79 (5R)	1.27 (11R)
	Older	49	1.00	0.16	0.63 (29L)	1.39 (48R)
	Young vs older		$P=0.86$	$P=0.0042$		
Area ratio	Young	50	1.32	0.15	1.03 (24L)	1.67 (17R)
	Older	46	1.19	0.35	0.45 (29R)	2.09 (37R)
	Young vs older		$P=0.059$	$P<0.0001$		

*Brackets identify the carotid bifurcations in Figures 2 and 3 at which the respective extrema occurred.

similarly revealed no significant differences between the interindividual variations within these 2 groups, whereas unpaired *t* tests revealed significant differences only between the means of the ECA:ICA diameter ratio ($P=0.0015$). Therefore, we conclude that our data, despite being drawn from a relatively small sample, is representative of a broader

population. On the other hand, we note that such small sample sizes would be inadequate for elucidating relationships between vessel geometry and baseline demographics, which explains why we were unable to confirm a significant effect of sex²¹ and plaque burden⁹ on vessel geometry in our older group.

TABLE 2. Reproducibility of Geometric Parameters

Geometric Parameter	Mean	SD*
Bifurcation angle	61.5°	4.1°
ICA angle	28.4°	4.6°
ICA planarity	9.1°	4.3°
CCA tortuosity	0.014	0.005
ICA tortuosity	0.065	0.009
ICA:CCA	0.74	0.03
ECA:CCA	0.67	0.04
ECA:ICA	0.91	0.04
Area ratio	1.01	0.08

*Mean intraindividual SD calculated as the square root of the average within-subject variance.

Implications for the Geometric Risk Hypothesis

The inevitable implication of our findings is that interindividual variation in the geometry of the carotid bifurcation increases with aging and/or disease. Although it is difficult to separate these 2 factors, we do note that data from the ECST study showed similar levels of variation in patients with <30% stenosis and patients with no disease evident on angiography. From this we infer that geometric variability does not necessarily increase with the progression of mild disease, for otherwise we would expect these groups to have different levels of interindividual variation. Changes in carotid bifurcation geometry are, therefore, more likely to reflect the influence of early, angiographically silent disease or, simply, the vascular aging process. Our data do not distinguish between these possibilities, although the near-significant effect of total plaque area on the ICA:CCA

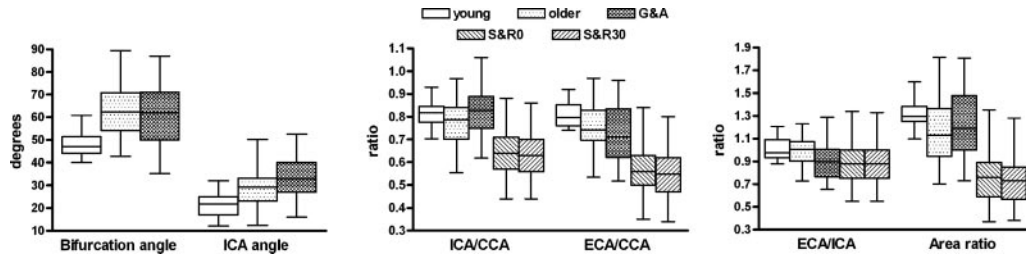


Figure 4. Comparison of data from young and older groups with data from Goubergrits et al.^{16,17} (G&A) and Schulz and Rothwell¹⁰ for ECST subjects with no disease (S&R0) and <30% stenosis (S&R30). Boxes and whiskers identify interquartile and 95% ranges, respectively. Horizontal lines within boxes identify medians for young, older, and G&A groups, and means for the S&R0 and S&R30 groups (medians for these data were not provided).

diameter and bifurcation area ratios hints that the former may be the case. Moreover, we note that the only longitudinal study of geometric risk of atherosclerosis concluded that, for the femoral artery, changes in vessel tortuosity preceded (angiographically defined) atherosclerosis development.²² At the very least, these observations suggest that the geometry of the carotid bifurcation in youth does not necessarily anticipate its future state.

Alternatively, it is possible that the modest interindividual differences in the carotid bifurcation geometries of young adults may still give rise to a geometric risk for atherosclerosis. This is because, for all of the focus on geometry, it is the local hemodynamic forces induced by geometry that provide the mechanistic link underpinning the geometric risk hypothesis. The sensitivity of local hemodynamic forces to geometry is well appreciated in a qualitative sense but not sufficiently well understood quantitatively to know what “major” or “modest” interindividual variations in geometry mean in terms of interindividual variations in the hemodynamic parameters relevant to atherosclerosis. (This is poised to change given recent developments in the area of computational fluid dynamics.²³) Still, our reproducibility data indicate that inherent variability in the noninvasive characterization of carotid bifurcation geometry by MRI is roughly of the same order as interindividual variability in the young group. Although this does confirm that the levels of interindividual variations observed in the present study—and, especially, the significant differences between interindividual variations within the 2 groups—are real and not merely a reflection of inherent measurement variability, it does suggest a lower bound, ≈30 years old, on the age at which geometric risk could be detected practically.

Summary

Our findings clearly demonstrate that interindividual variations in the geometry of the carotid bifurcation increase significantly with aging or early atherosclerotic disease progression. They do not, however, prove or disprove the idea that an individual’s geometry may predict the development and progression of atherosclerosis. Rather, they point to a more complex interrelationship among vascular geometry, local hemodynamics, vascular aging, and atherosclerosis, the elucidation of which will almost certainly require prospective studies.

We have shown here how the combination of noninvasive imaging and 3D image processing may be used to character-

ize vessel geometry in an objective and reproducible manner; and, so, with the increasing use of MR angiography, such prospective studies should be possible, especially in the 30- to 60-year-old age bracket when geometric variations appear to evolve. With this in mind, we have placed our geometric characterization tools in the public domain²⁴ with the hope of encouraging the standardization of geometric definitions, a step we believe will be crucial for future large-scale studies and meta-analyses aimed at identifying local factors predictive of successful vascular aging.

Acknowledgments

This work was supported by grants MOP-62934 (D.A.S.) and GR-14973 (B.K.R.) from the Canadian Institutes of Health Research and grant NA-4990 (J.D.S.) from the Heart and Stroke Foundation of Ontario. D.A.S. and B.K.R. acknowledge the support of a Heart and Stroke Foundation Career Investigator Award and the Barnett-Ivey-HSFO Research Chair, respectively. The work of L.A. was supported in part by a fellowship from the Mario Negri Institute for Pharmacological Research. We thank Carlotta Rossi and Dr Guido Bertolini from the Laboratory of Clinical Epidemiology, Mario Negri Institute, for advice regarding the statistical analysis. Guarantor of integrity of entire study, D.A.S.; study concept/design, J.B.T., L.A., J.D.S., B.K.R., D.A.S.; subject recruitment, J.B.T., J.D.S.; literature research, J.B.T., S.L.C., D.A.H.S.; data acquisition, J.B.T.; data analysis/interpretation, J.B.T., L.A., S.L.C., J.S.M., D.A.H.S., D.A.S.; statistical analysis, L.A.; manuscript preparation, J.B.T., L.A., D.A.S.; manuscript definition of intellectual content, J.B.T., L.A., D.A.S.; manuscript editing and revision/review, J.B.T., L.A., J.S.M., D.A.H.S., J.D.S., B.K.R., D.A.S.; and manuscript final version approval, all authors.

References

1. Malek AM, Alper SL, Izumo S. Hemodynamic shear stress and its role in atherosclerosis. *J Am Med Assoc.* 1999;282:2035–2042.
2. Friedman MH, Deters OJ, Mark FF, Barger CB, Hutchins GM. Arterial geometry affects hemodynamics. A potential risk factor for atherosclerosis. *Atherosclerosis.* 1983;46:225–231.
3. Harrison MJG, Marshall J. Does the geometry of the carotid bifurcation affect its predisposition to atheroma? *Stroke.* 1983;14:117–118.
4. Spelde AG, de Vos RA, Hoogendam IJ, Heethaar RM. Pathological-anatomical study concerning the geometry and atherosclerosis of the carotid bifurcation. *Eur J Vasc Surg.* 1990;4:345–348.
5. Fisher M, Fieman S. Geometric factors of the bifurcation in carotid atherogenesis. *Stroke.* 1990;21:267–271.
6. Smedby O. Geometric risk factors for atherosclerosis in the aortic bifurcation: a digitized angiography study. *Ann Biomed Eng.* 1996;24:481–488.
7. Ding Z, Biggs T, Seed WA, Friedman MH. Influence of the geometry of the left main coronary artery bifurcation on the distribution of sudanophilia in the daughter vessels. *Arterioscler Thromb Vasc Biol.* 1997;17:1356–1360.
8. Smedby O. Geometrical risk factors for atherosclerosis in the femoral artery: a longitudinal angiographic study. *Ann Biomed Eng.* 1998;26:391–397.

9. Sitzer M, Puac D, Buehler A, Steckel DA, Von Kegler S, Markus HS, Steinmetz H. Internal carotid artery angle of origin: a novel risk factor for early carotid atherosclerosis. *Stroke*. 2003;34:950–955.
10. Schulz UG, Rothwell PM. Major variation in carotid bifurcation anatomy: a possible risk factor for plaque development? *Stroke*. 2001;32:2522–2529.
11. Spence JD, Eliasziw M, DiCicco M, Hackam DG, Galil R, Lohmann T. Carotid plaque area: a tool for targeting and evaluating vascular preventive therapy. *Stroke*. 2002;33:2916–2922.
12. Ladak HM, Thomas JB, Mitchell JR, Rutt BK, Steinman DA. A semi-automatic technique for measurement of arterial wall from black blood MRI. *Med Phys*. 2001;28:1098–1107.
13. Ladak HM, Milner JS, Steinman DA. Rapid three-dimensional segmentation of the carotid bifurcation from serial MR images. *J Biomech Eng*. 2000;122:96–99.
14. Steinman DA, Thomas JB, Ladak HM, Milner JS, Rutt BK, Spence JD. Reconstruction of carotid bifurcation hemodynamics and wall thickness using computational fluid dynamics and MRI. *Magn Reson Med*. 2002;47:149–159.
15. Antiga L, Steinman DA. Robust and objective decomposition and mapping of bifurcating vessels. *IEEE Trans Med Imaging*. 2004;23:704–713.
16. Goubergrits L, Affeld K, Fernandez-Britto J, Falcon L. Atherosclerosis in the human common carotid artery. A morphometric study of 31 specimens. *Pathol Res Pract*. 2001;197:803–809.
17. Goubergrits L, Affeld K, Fernandez-Britto J, Falcon L. Geometry of the human common carotid artery. A vessel cast study of 86 specimens. *Pathol Res Pract*. 2002;198:543–551.
18. Thomas JB, Milner JS, Rutt BK, Steinman DA. Reproducibility of image-based computational fluid dynamics models of the human carotid bifurcation. *Ann Biomed Eng*. 2003;31:132–141.
19. Thomas JB, Jong L, Spence JD, Wasserman BA, Rutt BK, Steinman DA. Anthropometric data for MR imaging of the carotid bifurcation. *J Magn Reson Imaging*. 2005;21:845–849.
20. Forster FK, Chikos PM, Frazier JS. Geometric modeling of the carotid bifurcation in humans: implications in ultrasonic Doppler and radiologic investigations. *J Clin Ultrasound*. 1985;13:385–390.
21. Schulz UG, Rothwell PM. Sex differences in carotid bifurcation anatomy and the distribution of atherosclerotic plaque. *Stroke*. 2001;32:1525–1531.
22. Smedby O, Bergstrand L. Tortuosity and atherosclerosis in the femoral artery: what is cause and what is effect? *Ann Biomed Eng*. 1996;24:474–480.
23. Steinman DA. Image-based computational fluid dynamics: A new paradigm for monitoring hemodynamics and atherosclerosis. *Curr Drug Targets Cardiovasc Hematol Disord*. 2004;4:183–197.
24. <http://vmtk.sourceforge.net>. Accessed October 4, 2005.